

Neurofibromatosis type 1: Diffusion weighted imaging findings of brain

Alpay Alkan^{a,*}, Ahmet Sigirci^a, Ramazan Kutlu^a, Hamdi Ozcan^b, Gulnur Erdem^a,
Mehmet Aslan^c, Ozkan Ates^d, Cengiz Yakinci^c, Mucahit Egri^e

^a Department of Radiology, Turgut Ozal Medical Center, Inonu University School of Medicine, 44069 Malatya, Turkey

^b Department of Dermatology, Inonu University School of Medicine, Malatya, Turkey

^c Department of Pediatrics, Inonu University School of Medicine, Malatya, Turkey

^d Department of Neurosurgery, Inonu University School of Medicine, Malatya, Turkey

^e Department of Public Health, Inonu University School of Medicine, Malatya, Turkey

Received 29 March 2005; received in revised form 11 May 2005; accepted 13 May 2005

Abstract

Purpose: The purposes of this study were to evaluate the differences in apparent diffusion coefficient (ADC) values between infra and supratentorial unidentified bright objects (UBOs), between UBOs and normal appearing side (NAS, contralateral regions of the UBOs and/or normal appearing region without UBOs) in the neurofibromatosis type 1 patients (NF1) and control group and also to investigate correlation between age and ADC values.

Methods: A total of 30 patients and 26 healthy controls were included. The MRI examination consisted of routine imaging and diffusion weighted imaging (DWI). Seven distinct locations (frontal, parieto-occipital and cerebellar white matter, globus pallidum, thalamus, hippocampus, and midbrain) were selected for the analysis. The ADC values were calculated directly from these automatically generated ADC maps with ROI.

Results: The ADC values of UBOs were significantly increased in cerebellar white matter, hippocampus, globus pallidum, midbrain, and thalamus when compared with NAS and control group. There were statistically significant differences between NAS and control group in the ADC values obtained from hippocampus and thalamus. There were statistically significant differences between supra and infratentorial UBOs in ADC values. There was a negative correlation between age and the ADC values obtained from normal appearing midbrain, hippocampus, thalamus, and globus pallidum.

Conclusion: ADC values both in UBOs and in the normal appearing locations as hippocampus and thalamus were detected to be higher in the patients with NF1. The detection of lesions might be independent of MRI appearance in NF1, i.e. although the brain is affected, MRI appearance may be normal. Therefore, DWI and ADC values should also be utilized in the delineation of brain involvement of NF1 patients. © 2005 Elsevier Ireland Ltd. All rights reserved.

Keywords: Neurofibromatosis type 1; Diffusion magnetic resonance imaging; Brain

1. Introduction

Neurofibromatosis type 1 (NF1), also known as von Recklinghausen disease, is a neurocutaneous syndrome. It is a genetic disease in humans, inherited by a gene located in chromosome 17, affecting one in 3000–4000 individuals [1–3].

MRI has been extensively used in the evaluation of patients with NF1. Parenchymal lesions appear as focal

areas of increased signal intensity on T2-weighted images, and are common feature of this disease [1,3–5]. Globus pallidum, brainstem, thalamus, cerebellum, and subcortical white matter are the most commonly involved sites [1–4,6]. These focal parenchymal lesions, which have also been called unidentified bright objects (UBOs) are observed in 40–93% of children with NF1 [7]. Their nature is still not known exactly although they may include the areas of heterotopia, gliosis, low-grade astrocytomas, atypical glial infiltrates, foci of microcalcifications, dysplasias, and spongiform or vacuolar change of the white matter due to intramyelinic edema [8–10].

* Corresponding author. Tel.: +90 422341 0660x5710;
fax: +90 422 341 0834.

E-mail address: aalkan@inonu.edu.tr (A. Alkan).

Diffusion weighted imaging (DWI) provides important information in evaluating the structure of tissues and intracranial lesions. The random motion of water molecules, also known as Brownian motion, is restricted only by their local environment, such as cellular structures, cell walls, and orientation of the local tissue bundle [8]. The net diffusion of the molecules is referred to as the apparent diffusion coefficient (ADC). The finding of brain diffusion abnormalities in patient with NF1 might represent evidence of microstructural abnormalities [11].

The purposes of this study were to evaluate the differences in ADC values between infra and supratentorial UBOs, between UBOs and normal appearing side (NAS, contralateral regions of the UBOs and/or normal appearing region without UBOs) in the patients and control group and also to investigate correlation between age and ADC values.

2. Materials and methods

A total of 30 consecutive patients (13 females, 17 males, age range: 5–64 years, mean age: 23.2 ± 14.9) who were referred to our neuroradiology department and had the diagnosis of NF1 based on standard clinical criteria [12] and 26 healthy volunteers (12 females, 14 males, age range: 6–48 years, mean age: 23.1 ± 12.6) were included in this study. None of the patients and controls was sedated. This study was approved by the hospital Ethics Committee.

The MRI examination consisted of routine imaging and DWI. MRI was performed on a 1.5-T system (Philips, Gyroscan Intera Master, Best, The Netherlands). The evaluated imaging sequences were fluid-attenuated inversion-recovery (FLAIR) T2 weighted fast spin echo (TR: 6000, TE: 110, TI: 2000 ms), T2 weighted fast spin echo (TR: 4530, TE: 100 ms), and T1 weighted images (TR: 560, TE: 15 ms). T1-weighted sequence was repeated in coronal and axial plane after i.v. application of Gd-DTPA. MRI of the brain were analyzed for number, size, and distribution of hyperintense lesions that were visible only on T2-weighted images and were characterized by lack of contrast enhancement or mass effect. These lesions were classified as “UBOs”.

For the DWI, single-shot echo-planar pulse sequence (TR: 4832 ms, TE: 81 ms, field of view 230 mm, matrix size 128×256 , slice thickness 7 mm, interslice gap 1 mm) was used in all patients and controls with two different b values (0 and 1000 s/mm^2). The diffusion gradients were applied along the three axes (x, y, z) simultaneously. The ADC maps were reconstructed with the commercially available software. We calculated directionally averaged ADC from ADC map, in circular regions of interest (ROI) drawn on the regions identified on the baseline T2-weighted $b=0 \text{ s/mm}^2$ images. In each patients and healthy controls, seven distinct neuroanatomic structures were selected for the analysis. The anatomic locations were chosen to represent the sites that are likely to appear abnormal at MR imaging in patients with NF1 [2–4,11]. The area of ROI's were 170 mm^2 in white matter

of frontal and parieto-occipital white matter, and hippocampus, 130 mm^2 in globus pallidum and thalamus, 100 mm^2 in cerebellar white matter and 70 mm^2 in midbrain.

All statistical analyses were performed using a commercially available SPSS release 11.0 software package (SPSS Inc., Chicago, IL). The results are presented as mean \pm standard deviation in order to facilitate comprehension of the tables. The measurements in all groups showed normal distribution with Kolmogorov–Smirnov test. One way analysis of variance (ANOVA) test was utilized for the comparison of ADC values among groups. Tukey HSD test was used for the assessment of differences in the ADC values for UBOs, NAS and control group. Pearson's correlation test was used to assess the correlation between age and the ADC values in the UBOs and NAS of cerebellar white matter, globus pallidum, thalamus, hippocampus, and midbrain. Mann–Whitney U two-tailed test was used to evaluate the differences in the ADC values of seven distinct locations between all patients ($n=30$) and control group and also in the ADC values between infratentorial and supratentorial UBOs. A p value below 0.05 was considered statistically significant.

3. Results

There was no significant difference in age between patients and control group.

Seventy-nine UBOs were found in the cerebellar white matter ($n=23$), hippocampus ($n=21$), globus pallidum ($n=19$), midbrain ($n=8$), and thalamus ($n=8$) with MRI.

The ADC values obtained from frontal, parieto-occipital and cerebellar white matter, globus pallidum, hippocampus, thalamus, and midbrain were significantly increased in patients ($n=30$) compared to control subjects ($p < 0.05$).

The ADC values of UBOs were significantly increased in cerebellar white matter, hippocampus, globus pallidum, midbrain, and thalamus when compared with NAS and control group ($p=0.000$ and 0.000) (Fig. 1).

There were statistically significant differences between NAS and control group in the ADC values obtained from hippocampus and thalamus (respectively, $p=0.01$ and 0.000) (Figs. 2 and 3).

There was statistically significant differences between supratentorial ($n=56$) and infratentorial ($n=23$) UBOs in ADC values ($1098 \pm 183 \times 10^{-6}$, $929 \pm 266 \times 10^{-6} \text{ mm}^2/\text{s}$, respectively) ($p=0.001$) (Table 1).

There were a negative correlation between age and the ADC values obtained from normal appearing midbrain, hippocampus, thalamus, and globus pallidum (respectively, $r=-0.4$, -0.5 , -0.5 , and -0.5).

4. Discussion

DWI is dependent on the random motion of water molecules, and offers an opportunity to evaluate the structural

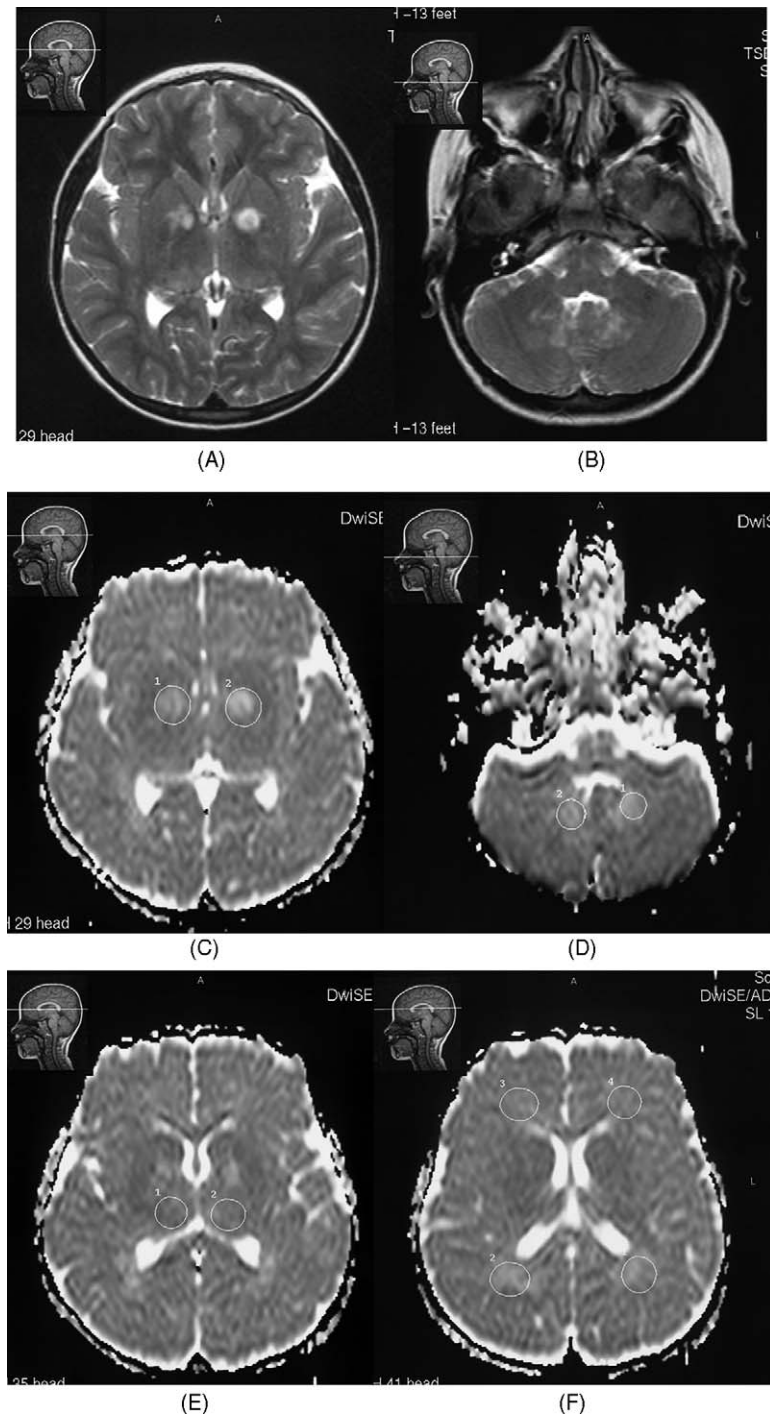


Fig. 1. An 11-year-old female with NF1. (A and B) Axial T2 weighted images (4530/100) show focal parenchymal lesions (UBOs) in bilateral globus pallidum and cerebellar white matter. (C and D) ADC maps reveal high signal intensity and ADC values in the bilateral globus pallidum (1056×10^{-6} and $1209 \times 10^{-6} \text{ mm}^2/\text{s}$), and cerebellar white matter (1061×10^{-6} and $1038 \times 10^{-6} \text{ mm}^2/\text{s}$). (E and F) ADC maps reveal high ADC values in the thalamus as NAS (1014×10^{-6} and $928 \times 10^{-6} \text{ mm}^2/\text{s}$), frontal (883×10^{-6} and $895 \times 10^{-6} \text{ mm}^2/\text{s}$) and parieto-occipital white matter (1041×10^{-6} and $1029 \times 10^{-6} \text{ mm}^2/\text{s}$).

characteristics of tissues [11]. DWI allows quantitative measurement of the water molecules in biologic tissues during the application of strong magnetic field gradients. Besides true diffusion images ($b = 1000 \text{ s/mm}^2$), ADC maps reveal signal differences between lesions and normal brain tissue. ADC reflects the structural properties of the cellular compartments

of the tissue studied and it provides a rotationally invariant measurement of the total diffusion of water within a tissue [13].

Existing pathologic data about NF1 have shown an association between UBOs and myelin vacuoles which may represent further evidence of a demyelinating process [10,11].

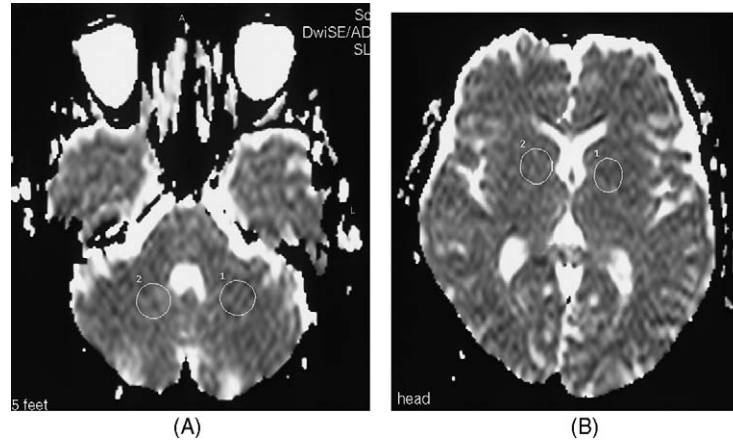


Fig. 2. A 38-year-old male patient without UBOs (NAS). (A and B) ADC maps reveal normal signal intensity and ADC values in the cerebellar white matter (717×10^{-6} and 727×10^{-6} mm^2/s) and globus pallidum (671×10^{-6} and 710×10^{-6} mm^2/s).

The hyperintense lesions could represent focally severe disease within a more widespread myelin disorder. Eastwood et al. reported that a myelin disturbance, such as diminished myelin amount, increased myelin turnover, or demyelina-

tion, is present in the brains of children having NF1 on DWI [11]. In demyelinating disease, the loss of normal myelin structure and the axonal loss lead to an expansion of the extracellular space which results in an increase in ADC

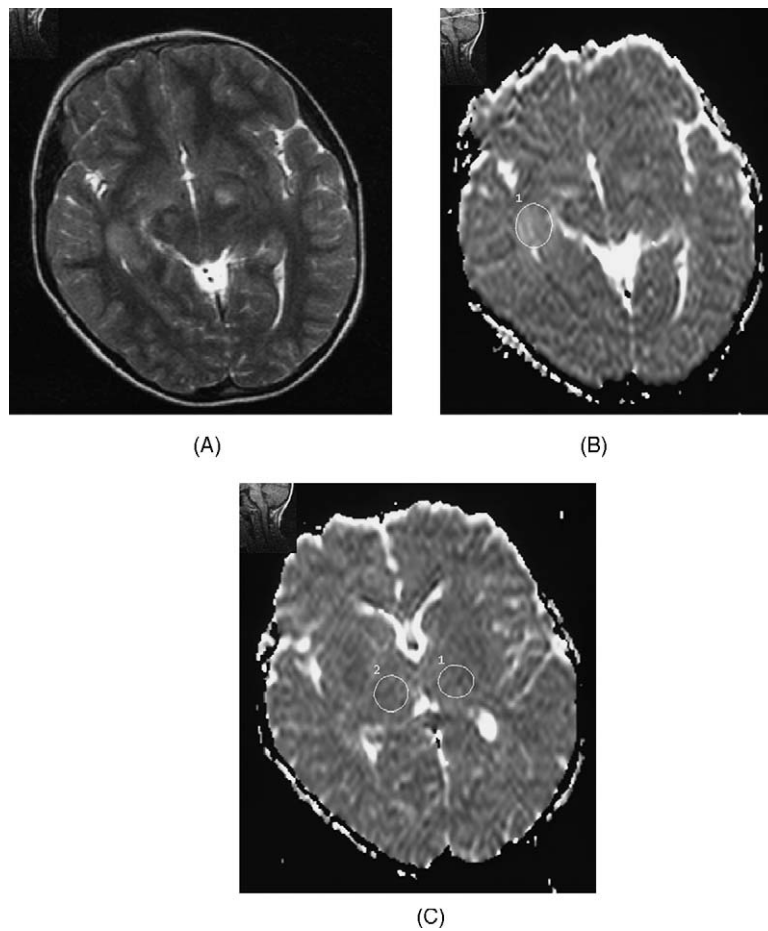


Fig. 3. A 10-year-old female with NF1. (A) Axial T2 weighted image (4530/100) shows focal parenchymal lesions (UBOs) in right hippocampus and left cerebral peduncle. (B) ADC map reveals high signal intensity and ADC value in the right hippocampus (1091×10^{-6} mm^2/s). (C) The ADC map shows high ADC values in the thalamus (NAS) (832×10^{-6} and 841×10^{-6} mm^2/s).

Table 1
Mean ADC values of patients with NF1

Groups	Mean ADC values ($\times 10^{-6}$ mm ² /s)						
	POWM	FWM	CWM	Globus pallidum	Thalamus	Hippocampus	Midbrain
UBOs	–	–	929 \pm 266 (n = 23)	1044 \pm 90 (n = 19)	1015 \pm 103 (n = 8)	1124 \pm 123 (n = 21)	1243 \pm 383 (n = 8)
NAS	–	–	728 \pm 42 (n = 37)	743 \pm 34 (n = 41)	800 \pm 56 (n = 52)	841 \pm 48 (n = 39)	721 \pm 70 (n = 22)
NF1 patients (n = 30)	908 \pm 109	794 \pm 53	843 \pm 152	839 \pm 152	828 \pm 97	940 \pm 158	860 \pm 307
Control (n = 26)	791 \pm 54	758 \pm 51	714 \pm 47	726 \pm 31	732 \pm 36	810 \pm 36	704 \pm 56

POWM: parieto-occipital white matter; FWM: frontal white matter; CWM: cerebellar white matter; UBOs: unidentified bright objects; NAS: normal appearing side; ADC: apparent diffusion coefficient.

[11,14]. The higher ADC values in the UBOs suggest that there is a relatively high molecular motion in these regions, compared to the normal brain parenchyma. In our study, increased ADC values in the UBOs of cerebellar white matter, hippocampus, globus pallidum, midbrain, and thalamus when compared to NAS and control group may represent a myelin disorder as demyelination. Meanwhile, the significant increase in ADC values in the supratentorial UBOs when compared with infratentorial ones may indicate more prominent demyelination in the supratentorial level. The ADC changes that observed in the supratentorial UBOs in our study were similar to those described in the literature [8]. The cellular composition of UBOs may change, with development of more myelin vacuoles, at a different rate [8]. In our study, the patients with NF1 that have normal appearing hippocampus and thalamus (NAS) on T2 weighted images were revealed significant increase in ADC values that may be due to residual lesions. However, ADC values that obtained from normal appearing globus pallidum, cerebellar white matter, and midbrain were similar both in the patients and control group.

UBOs are not generally seen in adults with NF1 and spontaneous regression, often in the second decade, has been reported [15,16]. Resolution of signal abnormalities on T2 weighted images with age may reflect change in water content within brain alterations [8,17]. The regression and resolution of UBOs may be explained with the NF-1 gene product, neurofibromin, which is mainly expressed in the nervous system in adults [18]. The relationship between age and ADC values of normal appearing midbrain, hippocampus, thalamus, and globus pallidum was significantly negative in our study. This finding could indicate the myelination, organization, and repair of myelin disorder.

5. Conclusion

The ADC values of UBOs were significantly increased in cerebellar white matter, hippocampus, globus pallidum, midbrain, and thalamus when compared with NAS and control group. Additionally, ADC values of NAS only in the hippocampus and thalamus were higher in the patients than control group. The detection of lesions might be independent of MRI appearance in NF1, i.e. although the brain is

affected, MRI appearance may be normal. Therefore, DWI and ADC values should also be utilized in the delineation of brain involvement of NF1 patients.

References

- [1] Pont MS, Elster AD. Lesions of skin and brain: modern imaging of the neurocutaneous syndromes. *AJR Am J Roentgenol* 1992;158:1193–203.
- [2] Alkan A, Sarac K, Kutlu R, et al. Proton MR spectroscopy features of normal appearing white matter in neurofibromatosis type 1. *Magn Reson Imaging* 2003;21(9):1049–53.
- [3] Alkan A, Kutlu R, Sigirci A, et al. MR spectroscopy in the differential diagnosis of focal brain lesions in neurofibromatosis type 1 patients. *Tani Girisim Radyol* 2003;9(2):166–70.
- [4] DiMario FJ, Ramsby G. Magnetic resonance imaging lesion analysis in neurofibromatosis type 1. *Arch Neurol* 1988;55:500–5.
- [5] Itoh T, Magnaldi S, White RM, et al. Neurofibromatosis type 1: the evolution of deep grey and white matter abnormalities. *Am J Neuroradiol* 1994;15:1513–9.
- [6] Molloy PT, Bilaniuk LT, Vaughan SN, et al. Brainstem tumors in patients with neurofibromatosis type 1. A distinct clinical entity. *Neurology* 1995;45:1897–902.
- [7] Steen RG, Taylor JS, Langston JW, et al. Prospective evaluation of the brain in asymptomatic children with neurofibromatosis type 1: relationship of macrocephaly to T1 relaxation changes and structural brain abnormalities. *AJNR Am J Neuroradiol* 2001;22(5):810–7.
- [8] Sheikh SF, Kubal WS, Anderson AW, Mutalik P. Longitudinal evaluation of apparent diffusion coefficient in children with neurofibromatosis type 1. *J Comput Assist Tomogr* 2003;27(5):681–6.
- [9] Inoue Y, Nemoto Y, Tashiro T, Nakayama K, Nakayama T, Daikokuya H. Neurofibromatosis type 1 and type 2: review of the central nervous system and related structures. *Brain Dev* 1997;19(1):1–12.
- [10] DiPaolo DP, Zimmerman RA, Rorke LB, Zackai EH, Bilaniuk LT, Yachnis AT. Neurofibromatosis type 1: pathological substrate of high-signal intensity foci in the brain. *Radiology* 1995;195:721–4.
- [11] Eastwood JD, Fiorella DJ, MacFall JF, DeLong DM, Provenzale JM, Greenwood RS. Increased brain apparent diffusion coefficient in children with neurofibromatosis type 1. *Radiology* 2001;219(2):354–8.
- [12] NIH consensus development conference. Neurofibromatosis conference statement. *Arch Neurol* 1988;45:575–8.
- [13] Caramia F, Pantano P, Di Legge S, et al. A longitudinal study of MR diffusion changes in normal appearing white matter of patients with early multiple sclerosis. *Magn Reson Imaging* 2002;20:383–8.
- [14] Bammer R, Fazekas F. Diffusion imaging in multiple sclerosis. *Neuroimaging Clin N Am* 2002;12(1):71–106.
- [15] Sevick RJ, Barkovich AJ, Edwards MSB, Koch T, Berg B, Lemberg T. Evaluation of white matter lesions in neurofibromatosis type 1: MR findings. *AJR Am J Roentgenol* 1992;159:171–5.

- [16] Kim G, Mehta M, Kucharczyk W, Blaser S. Spontaneous regression of a tectal mass neurofibromatosis 1. *AJNR Am J Neuroradiol* 1998;19:1137–9.
- [17] Menor F, Marti-Bonmati L, Arana E, Poyatos C, Cortina H. Neurofibromatosis type 1 in children: MR imaging and follow-up studies of central nervous system findings. *Eur J Radiol* 1998;26(2):121–31.
- [18] Leisti EL, Pyhtinen J, Poyhonen M. Spontaneous decrease of a pilocytic astrocytoma in neurofibromatosis type 1. *AJNR Am J Neuroradiol* 1996;17(9):1691–4.